Hallucigenia's head and the pharyngeal armature of early ecdysozoans

Martin R. Smith[1] and Jean-Bernard Caron[2,3]

[1]Department of Earth Sciences, University of Cambridge, Cambridge, CB2 3EQ, UK. <ms609@cam.ac.uk>

[2]Department of Natural History (Palaeobiology Section), Royal Ontario Museum, Toronto, ON M5S 2C6, Canada. <jcaron@rom.on.ca>

[3]Department of Ecology and Evolutionary Biology and Earth Sciences, University of Toronto, Toronto, ON M5S 3B2, Canada.

Keywords: *Hallucigenia*, Ecdysozoa, Panarthropoda, Onychophora, Lobopodia, Burgess Shale, Cambrian explosion.

The molecularly-defined clade Ecdysozoa[1] comprises the panarthropods (Euarthropoda, Onychophora, and Tardigrada) and the cycloneuralian worms (Nematoda, Nematomorpha, Priapulida, Loricifera, and Kinorhyncha). These disparate phyla are united by their means of moulting, but otherwise share few morphological characters – none of which has a meaningful fossilization potential. As such, the early evolutionary history of the group as a whole is largely uncharted. Here we redescribe the 508 million year old stem-group onychophoran *Hallucigenia sparsa*[2–6] from the mid-Cambrian Burgess Shale. We document an elongate head with a pair of simple eyes, a terminal buccal chamber containing a radial array of sclerotized elements, and a differentiated foregut that is lined with acicular teeth. The radial elements and pharyngeal teeth resemble the sclerotized circumoral elements and pharyngeal teeth expressed in tardigrades[7–9], stem-group euarthropods[10–12], and

cycloneuralian worms[13]. Phylogenetic results indicate that equivalent structures characterized the ancestral panarthropod and, seemingly, the ancestral ecdysozoan – demonstrating the deep homology of panarthropod and cycloneuralian mouthparts, and providing an anatomical synapomorphy for the ecdysozoan supergroup.

Although Cambrian ecdysozoans offer an unrivalled perspective on early ecdysozoan evolution[6,14], significant uncertainty surrounds the morphology of the ancestral ecdysozoan. One of the few areas of agreement is that this ancestor bore a pharynx lined with ectodermally-derived, periodically moulted cuticle[7] and opening at a terminal mouth[15].

In many ecdysozoan taxa, the pharynx is lined with sclerotized teeth [9,10,12,13,16], and the mouth is surrounded by circumoral elements. The typical cycloneuralian mouth is surrounded by a ring of spines[13]; the tardigrade mouth bears circumoral lamellae[11,14,17]; stem-group euarthropods (e.g. *Hurdia, Kerygmachela, Jianshanopodia*) exhibit various lamellae and plates[10–12]; and the onychophoran mouth is enclosed by pustular lips. These elements have formerly been regarded as homologous throughout Ecdysozoa[12,15,18–21]. However, the non-sclerotized lips of onychophorans are not strictly circumoral[22], and onychophorans conspicuously lack pharyngeal teeth[16]. This suggests two possibilities: (1), a foregut armature of circumoral elements and pharyngeal teeth did exist in the ancestral ecdysozoan, but was secondarily lost in onychophorans; or (2) homoplasious armatures arose independently in Panarthropoda (either once or twice, depending on panarthropod relationships[6,23]) and Cycloneuralia.

The earliest history of onychophorans is pivotal to this dilemma. The first scenario implies that foregut armature was present in the ancestral onychophoran, whereas under the second, onychophorans never had foregut armature. To reconstruct the ancestral configuration of the onychophoran foregut, we turn to the celebrated lobopodian

Hallucigenia sparsa[2–4], now regarded as a stem-group onychophoran[5,6]. Until now, this taxon's potential significance for early ecdysozoan evolution has been curtailed by uncertainty in its morphological interpretation: *Hallucigenia* has variously been reconstructed on its side, upside down, and back to front (Extended Data Table 1). New material (Supplementary Table 1) and high-resolution microscopic analysis reveals many anatomical features in *Hallucigenia* for the first time. In particular, robust carbonaceous elements occur around *Hallucigenia*'s mouth and along its pharynx, implying that the ancestral onychophoran – and seemingly the ancestral ecdysozoan – bore circumoral elements and pharyngeal teeth.

Hallucigenia's tubular body ranges from 10 mm to more than 50 mm in length (Extended Data Fig. 1a–c; Supplementary Table 2). It bears ten elongate ventrolateral appendages (Fig. 1a–e); the anterior eight are of uniform length, whereas the posterior two are progressively shorter (Fig. 1d–e; Extended Data Fig. 2a–c). The final pair of appendages is terminal, confirming the absence of a posterior extension of the trunk[4]. The third to tenth leg pairs are regularly spaced; the first, second and third leg pairs are twice as close together (Fig. 1a–b, e; Extended Data Figs. 1c, 3a–b, 4e, 5a). The anterior three pairs of appendages are 1.5–2.0 times narrower than the posterior seven, and lacked claws. These narrow appendages were flexible and long enough to reach the mouth (Fig. 1a, e–g; Extended Data Figs. 1c–d, 2d, 3a, 4a, 6e–f). The posterior seven appendages bear terminal claws: two claws are present on appendages four to eight, forming an acute angle (Fig. 1a–d, Extended Data Fig. 3c–d, g), whereas a single claw adorns appendages nine and ten.

Seven pairs of equally-spaced elongate spines occupy the dorsolateral pinnacles of the trunk, situated above the third to ninth appendage pairs (Fig. 1a–e). The spines in each pair are separated by 60–90° (Extended Data Figs. 1, 4, 7). Each spine is supported by a buttress of soft tissue which forms a hump-like swelling of the body wall and is particularly prominent in larger individuals (Fig. 1d; Extended Data Figs. 1a, c, e, 6). The spines are uniform in length, width, spacing and shape: they are not quite straight but curve slightly (3.5° ± 0.9°) posteriad. The spines are centrifugally arranged in lateral view: the more anterior spines tilt forwards, the rear spines tilt backwards. The construction of the spines and claws from stacks of nested elements has been reported elsewhere[5,6].

The character of the trunk changes markedly at the position of the first pair of spines. Behind this point, the trunk exhibits a uniform girth. (A linear relationship between trunk girth and body length indicates isometric growth; see Supplementary Table 2.) In front of the first spine pair, the trunk is a third narrower than the posterior trunk, with a bulbous anterior expansion evident in smaller specimens (Fig. 1a–e; Extended Data Figs. 1–8). The anterior trunk usually bends at its midpoint, orienting the mouth opening ventrally.

Approximately 500 µm from the anterior of the body and 100 µm from the sagittal axis lies a dorsal pair of convex carbonaceous impressions, reaching 200 µm in diameter, which we interpret as eyes (Fig. 2a–c, i–j; Extended Data Figs. 3, 5, 7, 8b–d, 8i–m). Their irregular surface (Fig. 2c; Extended Data Figs. 3e, 5f, 8j, 8m) argues against the presence of ommatidia; the eyes were presumably simple rather than compound. This seems to be consistent with the eyes of other lobopodians (Supplementary Note 1, trans. ser. 18).

Reflective or darker regions occur along the axes of well-preserved appendages and appear, in the manner typical of lobopod limbs[24], to represent extensions of the hydrostatic body cavity (Fig. 1e). A large ampulla-shaped structure that opens anteriad represents a buccal chamber or ‘mouth’ (Fig. 1f–g; Extended Data Figs. 1d, 2f–g, 4b, 4f, 8f–g), and is followed by a foregut that consistently occupies the central 50% of the anterior trunk (Fig. 1e; Extended Data Figs. 1d, 2f–g, 4, 6, 7, 8a, 8k). The foregut is darker than the surrounding tissue, conceivably indicating the presence of a cuticular lining. At the end of the head, the foregut widens into a broader, poorly preserved midgut (Fig. 1e; Extended Data Figs. 2b, 4, 6); the gut ends in a terminal anus (Extended Data Fig. 2b), through which decay fluids – represented by a darkly stained region of variable extent (Fig. 1b, e; Extended Data Figs. 2a–c, 3a–b, 6a–d) – were expelled. Preservation of the hindgut is inadequate to determine whether it was differentiated from the midgut.

From behind the buccal chamber to the first pair of appendages, the dorsal surface of the foregut lumen is lined with dozens of posterior-directed aciculae (Fig. 2g–l; Extended Data Fig. 4c–d). These robustly carbonaceous structures are 10 µm long and gently curved; their consistent size and orientation, uniform distribution, and absence elsewhere in the gut excludes the possibility that they represent gut contents; rather, they were biologically associated with the gut wall.

At the back of the buccal chamber, around 200 µm from the anterior termination of the trunk, lies a 250 µm-wide crescentic structure composed of multiple identical lamellae, each around 10 µm across and 60 µm long. Lamellae are evident in every structure that is preserved, and consistently display a radial arrangement (Fig. 2a–f, i–j, Extended Data Figs. 5c–d, 8j–m). The structure is preserved laterally; it originally constituted a ring of lamellae around the opening of the foregut.

Like the claws and spines, the radial lamellae preserve as discrete carbonaceous films – they were originally sclerotized, rather than representing soft tissue such as muscle, cuticular folds, or pigmentation, and they do not represent a taphonomic artefact. The lamellae are fundamentally unlike the modified pair of claws that form the jaws of modern onychophorans. Insofar as they are numerous, elongate, and sclerotized, and are arranged radially around the anterior opening of the foregut, the lamellae convincingly resemble the circumoral elements present in other ecdysozoans (see discussion in Supplementary Note 1, trans. ser. 9). To evaluate the evolutionary significance of this similarity we incorporated our observations (summarized in Fig. 3 and Supplementary Videos 1–2) into an updated phylogenetic matrix (Supplementary Data).

The reconstruction of character states through Fitch parsimony indicates that sclerotized circumoral elements were present in the ancestral ecdysozoan (Fig. 4; Supplementary Note 1, trans. ser. 9), supporting the homology between circumoral structures in Tardigrada[9,14] and stem-euarthropods[10,11,14,25] and the circumoral ('coronal') spines of cycloneuralians[13,20,26] (see discussion in Supplementary Notes 1 & 2, trans. ser. 9). Homology between the panarthropod pharynx and the cycloneuralian pharynx is corroborated by the presence of robust sclerotized teeth in the anterior pharynx (Fig. 4; Supplementary Note 1, trans. ser. 13), previously reported in extant cycloneuralians, euarthropods and tardigrades[9,13,16,27] and now also evident in stem-group onychophorans. The simple construction of the modern onychophoran foregut therefore reflects a secondary loss of cycloneuralian-like pharyngeal teeth and circumoral elements in the onychophoran stem lineage, and stands in marked contrast to the complex armoured foregut of the ancestral ecdysozoan.

References

1. Aguinaldo, A. M. *et al.* Evidence for a clade of nematodes, arthropods and other moulting animals. *Nature* **387,** 489–493 (1997).
2. Conway Morris, S. A new metazoan from the Cambrian Burgess Shale of British Columbia. *Palaeontology* **20,** 623–640 (1977).
3. Ramsköld, L. & Chen, J.-Y. in *Arthropod fossils and phylogeny* (ed. Edgecombe, G. D.) 107–150 (Columbia University Press, 1998).

4. Ramsköld, L. The second leg row of *Hallucigenia* discovered. *Lethaia* **25,** 221–224 (1992).

5. Caron, J.-B., Smith, M. R. & Harvey, T. H. P. Beyond the Burgess Shale: Cambrian microfossils track the rise and fall of hallucigeniid lobopodians. *Proc. R. Soc. B* **280,** 20131613 (2013).

6. Smith, M. R. & Ortega-Hernández, J. *Hallucigenia*'s onychophoran-like claws and the case for Tactopoda. *Nature* **514,** 363–366 (2014).

7. Dewel, R. A., Clark, W. H. J. & Dewell, R. A. Studies on the tardigrades. II. Fine structure of the pharynx of *Milnesium tardigradum* Doyère. *Tissue Cell* **5,** 147–159 (1973).

8. Dewel, R. A. & Eibye-Jacobsen, J. The mouth cone and mouth ring of *Echiniscus viridissimus* Peterfi, 1956 (Heterotardigrada) with comparisons to corresponding structures in other tardigrades. *Hydrobiologia* **558,** 41–51 (2006).

9. Guidetti, R. *et al.* Form and function of the feeding apparatus in Eutardigrada (Tardigrada). *Zoomorphology* **131,** 127–148 (2012).

10. Vannier, J., Liu, J., Lerosey-Aubril, R., Vinther, J. & Daley, A. C. Sophisticated digestive systems in early arthropods. *Nat. Comm.* **5,** 3641 (2014).

11. Budd, G. E. The morphology and phylogenetic significance of *Kerygmachela kierkegaardi* Budd (Buen Formation, Lower Cambrian, N Greenland). *Trans. R. Soc. Edinb. Earth Sci.* **89,** 249–290 (1998).

12. Daley, A. C., Budd, G. E., Caron, J.-B., Edgecombe, G. D. & Collins, D. H. The Burgess Shale anomalocaridid *Hurdia* and its significance for early euarthropod evolution. *Science* **323,** 1597–1600 (2009).

13. Conway Morris, S. Fossil priapulid worms. *Spec. Pap. Pal.* **20,** (1977).

14. Budd, G. E. Tardigrades as 'stem-group arthropods': the evidence from the Cambrian fauna. *Zool. Anz.* **240,** 265–279 (2001).

15. Eriksson, B. J. & Budd, G. E. Onychophoran cephalic nerves and their bearing on our understanding of head segmentation and stem-group evolution of Arthropoda. *Arthr. Struc. Dev.* **29,** 197–209 (2000).

16. Elzinga, R. J. Microspines in the alimentary canal of Arthropoda, Onychophora, Annelida. *Int. J. Ins. Morph. Emb.* **27,** 341–349 (1998).

17. Dewel, R. A. & Dewel, W. C. The brain of *Echiniscus viridissimus* Peterfi, 1956 (Heterotardigrada): A key to understanding the phylogenetic position of tardigrades and the evolution of the arthropod head. *Zool. J. Linn. Soc.* **116,** 35–49 (1996).

18. Waggoner, B. Los comienzos de la historia evolutiva de los artrópodos: ¿qué nos pueden contar los fósiles? / The earliest evolutionary history of arthropods: what can the fossils tell us? *Boletín la Soc. Entomológica Aragon.* **26,** 115–131 (1999).

19. Hou, X.-G. *et al. Anomalocaris* and other large animals in the lower Cambrian Chengjiang fauna of southwest China. *GFF* **117,** 163–183 (1995).

20. Conway Morris, S. & Peel, J. S. New palaeoscolecidan worms from the Lower Cambrian: Sirius Passet, Latham Shale, and Kinzers Shale. *Acta Pal. Pol.* **55,** 141–156 (2010).

21. Rota-Stabelli, O. *et al.* A congruent solution to arthropod phylogeny: phylogenomics, microRNAs and morphology support monophyletic Mandibulata. *Proc. R. Soc. B* **278,** 298–306 (2011).

22. Martin, C. & Mayer, G. Neuronal tracing of oral nerves in a velvet worm—implications for the evolution of the ecdysozoan brain. *Front. Neuroanat.* **8,** 7 (2014).

23. Dunn, C. W., Giribet, G., Edgecombe, G. D. & Hejnol, A. Animal phylogeny and its evolutionary implications. *Annu. Rev. Ecol. Evol. Syst.* **45,** 371–395 (2014).

24. Liu, J. *et al.* New observations of the lobopod-like worm *Facivermis* from the Early Cambrian Chengjiang Lagerstätte. *Chin. Sci. Bull.* **51,** 358–363 (2006).

25. Daley, A. C. & Bergström, J. The oral cone of *Anomalocaris* is not a classic ‘peytoia’. *Naturwissenschaften* **99,** 501–504 (2012).

26. Maas, A., Huang, D., Chen, J.-Y., Waloszek, D. & Braun, A. Maotianshan-Shale nemathelminths — morphology, biology, and the phylogeny of Nemathelminthes. *Palaeogeogr. Palaeoclimatol. Palaeoecol.* **254,** 288–306 (2007).

27. Kristensen, R. M. Loricifera, a new phylum with Aschelminthes characters from the meiobenthos. *Zeitschrift für Zool. Syst. und Evol.* **21,** 163–180 (1983).

Supplementary information is linked to the online version of the paper at www.nature.com/nature.

Acknowledgments. We are grateful to three referees for detailed and thoughtful comments on the manuscript. We thank Doug Erwin, Mark Florence and Scott Whittaker (NMNH) for access to material and assistance with electron microscopy, and Kimberly Meechan for assistance with data collection. ROM specimens were collected under Parks Canada Research and Collection permits to Desmond Collins. TNT is made available with the sponsorship of the Willi Hennig Society. Funding for this research was provided by Clare College, Cambridge (MS), NSERC Discovery Grant #341944 (JBC) and the ROM DMV Acquisition and Research Fund and Endowment Fund (JBC). This is ROM Burgess Shale project number 60.

Author contributions. MRS performed data analysis; both authors examined and imaged material and contributed to the writing of the manuscript.

Author information. The authors declare no competing financial interests.

Reprints and permissions information is available at www.nature.com/reprints.

Correspondence should be addressed to ms609@cam.ac.uk.

Figure 1: Optical images of *Hallucigenia sparsa* from the Burgess Shale (anterior to the left). **a**, ROM 62269 (see also Extended Data Fig. 5); **b**, ROM 63142, SEM images are provided in Fig. 2g–l and Extended Data Fig. 3c; **c**, ROM 63051; see also Extended Data Fig. 3b, d–g; **d**, ROM 63146; high magnification images of the head are provided in Fig. 2a–f and Extended Data Fig. 7; **e**, NMNH 198658; see also Extended Data Fig. 2b–c; **f–g**, anterior section of ROM 57168; see also Extended Data Fig. 1c–e.

Acronyms for all figures: A = appendages, Ac = aciculae, An = anus, Bc = buccal chamber, C = claw, Df = decay fluids, E = eyes, F = foregut, G = gut, l = left, Mo = mouth opening, Cs = circumoral structure, Ce = circumoral elements, r = right, S = spines, $A_{1–n}$ or $S_{1–n}$ = order of A or S from front to back. Dotted white lines identify areas enlarged in Fig. 2 and Extended Data Figures, as denoted in captions. Unbroken white lines in b–d represent edges of the composite images of both parts and counterparts superimposed together. Black and white arrowhead denotes images flipped horizontally. Scale bars = 5 mm (a–e), 0.5 mm (f–g).

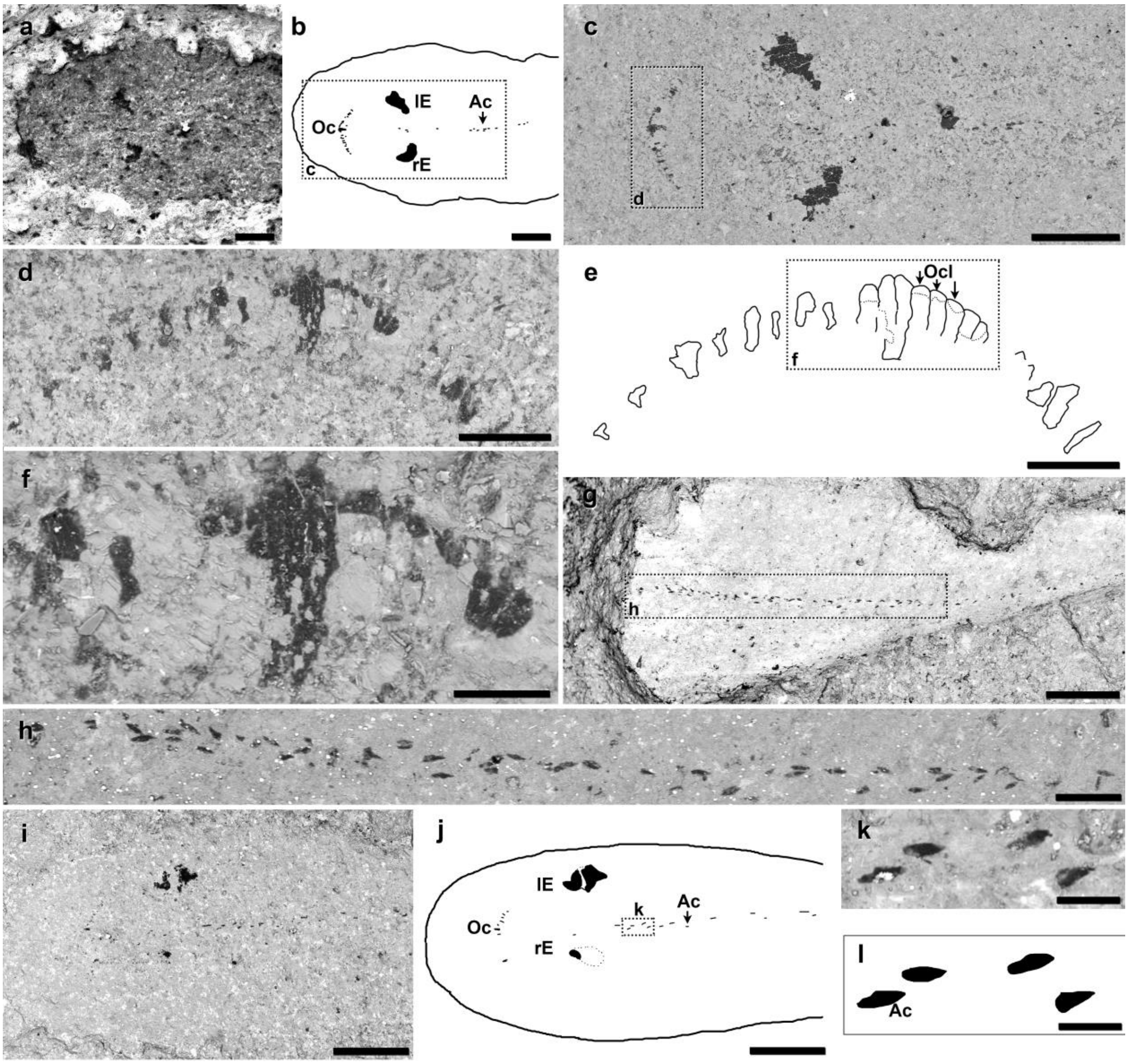

Figure 2: Scanning electron micrographs of the head region of *Hallucigenia sparsa* from the Burgess Shale. Anterior to the left except d–f, anterior to top of page. **a–f**, ROM 63146 (see Fig. 1d) with sketches of anterior region (b) and mouth plates (e); **g–l**, ROM 63142, part (g–h) and counterpart (i–l) showing aciculae. Acronyms and symbols as in Fig. 1. Detector mode: a, secondary electron; c–k, backscatter. Scale bars = 200 μm (a–c, g, i–j), 50 μm (d–e, h), 20 μm (f, k–l).

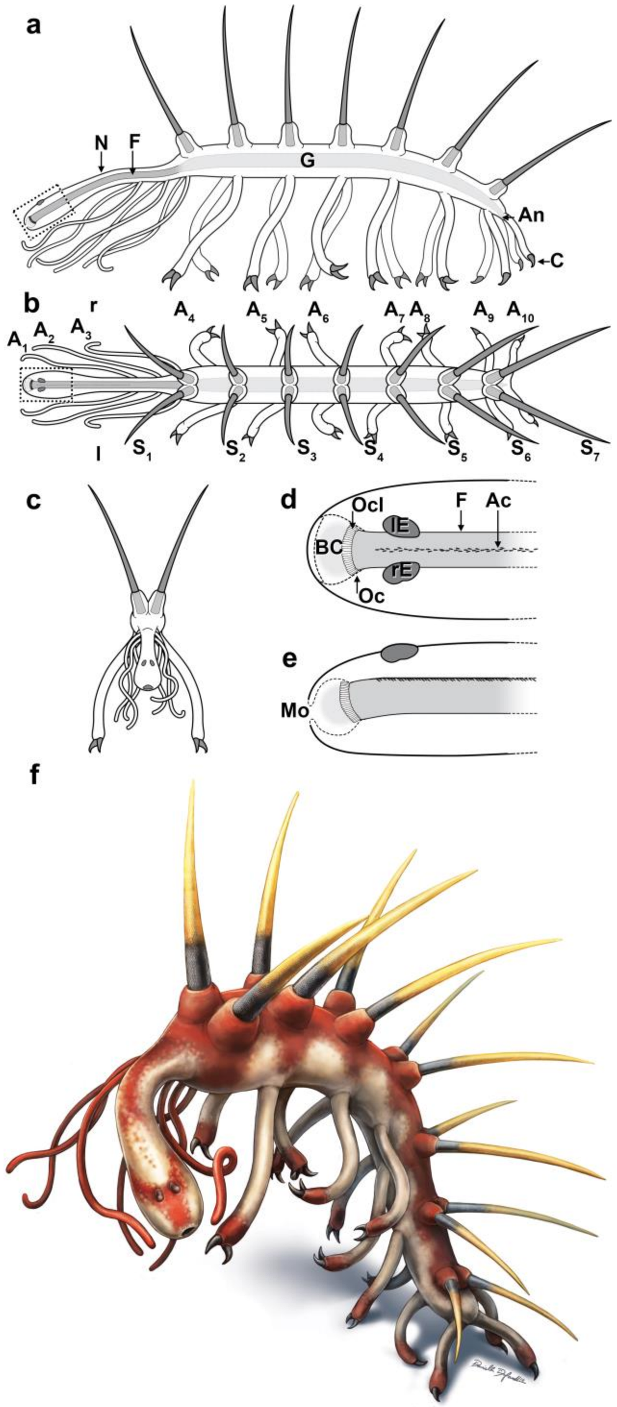

Figure 3: Anatomical drawings of *Hallucigenia sparsa* from the Burgess Shale. **a**, lateral profile; **b**, dorsal profile; **c**, frontal profile; **d–e**, head in dorsal (d) and lateral (e) views; **f**, full anatomical reconstruction. Drawings by Danielle Dufault. Acronyms as in Fig. 1.

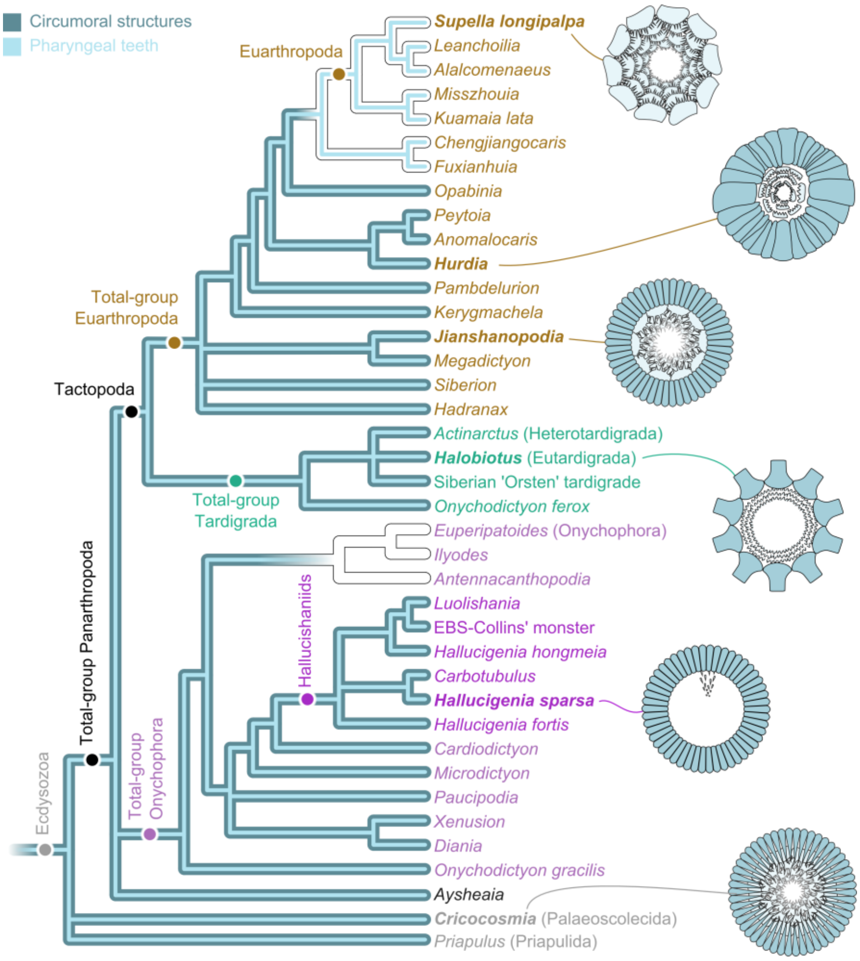

Figure 4: Ecdysozoan phylogeny, showing most parsimonious character distribution of circumoral structures (dark blue) and pharyngeal teeth (light blue). Fitch parsimony indicates the presence of both these structures in the ancestral ecdysozoan; a scenario positing multiple independent innovations of this armature would be less parsimonious. Topology shown denotes the strict consensus of all most parsimonious trees recovered under implied weights with concavity constant (*k*) between 0.46 and 211, after the removal of *Orstenotubulus*. The 'hallucishaniid' clade – diagnosed by a swollen head, dorsal spines, and the differentiation of the anterior trunk and trunk appendages – includes luolishaniids, *Orstenotubulus* and *Carbotubulus* within a paraphyletic '*Hallucigenia*'. Illustrated taxa are in bold type; see discussion of trans. ser. 9 & 13 in Supplementary Note 1. For phylogenetic data and full results see Supplementary Data.

Methods

Fossil materials. Materials are deposited at the Royal Ontario Museum, Toronto (ROM) and the Smithsonian Institution National Museum of Natural History, Washington DC (NMNH). Sediment covering parts of certain ROM specimens was manually removed using a tungsten-tipped micro-engraving tool. Specimens were photographed under various lighting conditions including dark- and bright-field illumination and polarized light, and imaged by backscatter and secondary electron microscopy under variable pressure.

Taphonomic considerations. As with other Burgess Shale organisms[28,29], *Hallucigenia sparsa* exhibits various degrees of pre- and post-burial decay, ranging from disarticulated specimens represented only by pairs of decay-resistant spines (Extended Data Fig. 9a) through partly disarticulated specimens retaining parts of the body (Extended Data Fig. 9b) to complete specimens, whose curled appendages and trunks are consistent with post-mortem contraction following rapid burial of live organisms (Fig. 1a–e; Extended Data Figs. 1–8). Consequently, the widths of the trunk and appendages are subject to slight taphonomic variation within and between specimens (e.g. Fig. 1). The full length of the body and appendages, where preserved, is typically buried within the matrix and is difficult to prepare mechanically.

Phylogenetic analysis. Phylogenetic analysis was conducted using the methods of Smith & Ortega-Hernández[6]; in summary, parsimony analysis was performed in TNT[30] under a range of weighting parameters, with Goloboff's concavity constant[31] ranging from k = 0.118 to 211, and under equal weights ($k = \infty$). Code is available in the Supplementary Data. *Orstenotubulus* (80% tokens 'ambiguous' or 'inapplicable') was identified as a wildcard taxon with an unconstrained position within the hallucishaniids; to improve resolution it is omitted from the strict consensus trees presented in the main manuscript.

Additional references

28. Conway Morris, S. & Caron, J.-B. *Pikaia gracilens* Walcott, a stem-group chordate from the Middle Cambrian of British Columbia. *Biol. Rev.* **87,** 480–512 (2012).
29. Smith, M. R. Nectocaridid ecology, diversity and affinity: early origin of a cephalopod-like body plan. *Paleobiology* **39,** 297–321 (2013).
30. Goloboff, P. A., Farris, J. S. & Nixon, K. C. TNT, a free program for phylogenetic analysis. *Cladistics* **24,** 774–786 (2008).
31. Goloboff, P. A. Estimating character weights during tree search. *Cladistics* **9,** 83–91 (1993).
32. Walcott, C. D. Cambrian Geology and Paleontology II, no. 5. Middle Cambrian annelids. *Smithson. Misc. Collect.* **57,** 109–144 (1911).
33. Ramsköld, L. & Hou, X.-G. New early Cambrian animal and onychophoran affinities of enigmatic metazoans. *Nature* **351,** 225–228 (1991).
34. Hou, X.-G. & Bergström, J. Cambrian lobopodians–ancestors of extant onychophorans? *Zool. J. Linn. Soc.* **114,** 3–19 (1995).
35. Steiner, M., Hu, S.-X., Liu, J. & Keupp, H. A new species of *Hallucigenia* from the Cambrian Stage 4 Wulongqing Formation of Yunnan (South China) and the structure of sclerites in lobopodians. *Bull. Geosci.* **87,** 107–124 (2012).

Extended Data legends

Extended Data Table 1: Interpretations of *Hallucigenia* through time.

Extended Data Figure 1: *Hallucigenia sparsa* from the Burgess Shale. **a–b**, largest (a, ROM 57169) and smallest (b, ROM 62093) specimens, to the same scale; **c**, ROM 57168, with enlargements of the anterior (**d**) and mid-trunk (**e**). Acronyms as in Fig. 1. Scale bars = 5 mm

Extended Data Figure 2: *Hallucigenia sparsa* from the Burgess Shale. **a**, ROM 63139, showing posterior body termination; **b–c**, NMNH 198658, showing posterior termination (see also Fig. 1e); **d–g**, ROM 63143: e, enlargement of region marked in d; f–g: backscatter SEMs of regions marked in e. Acronyms as in Fig. 1. Scale bars = 5 mm (a–d), 1 mm (e), 0.5 mm (f), 0.1 mm (g).

Extended Data Figure 3: *Hallucigenia sparsa* from the Burgess Shale. **a, c**, ROM 63142: a, composite image incorporating part and counterpart of the entire specimen; c, claw pair; **b, d–g**, ROM 63051: b, composite image incorporating part and counterpart of the entire specimen; d, anterior section; e–f, eyes; g, claw pair. c–e are backscatter electron micrographs.. Acronyms as in Fig. 1. Scale bars = 5 mm (a–b), 500 µm (d), 50 µm (c, f–g), 20 µm (e).

Extended Data Figure 4: *Hallucigenia sparsa* from the Burgess Shale. **a–d**, ROM 61513; a, entire specimen; b–d, enlargements of anterior region, showing mouth opening, aciculae and eyes; mouth opening to right in b, to left in c, d; **e–f**, ROM 61143; anterior region marked in e is enlarged in f. Acronyms as in Fig. 1. Scale bars = 5 mm (a, e), 1 mm (b, f), 200 µm (c), 20 µm (d).

Extended Data Figure 5: *Hallucigenia sparsa* (ROM 62269) from the Burgess Shale. **a**, part; **b**, counterpart, anterior section, showing eyes; **c–d**, eyes and mouthparts (backscatter SEM); **e–f**, detail of eyes (counterpart). Acronyms as in Fig. 1. Scale bars = 1 mm (a–b), 200 μm (e), 100 μm (c–d), 20 μm (f).

Extended Data Figure 6: *Hallucigenia sparsa* from the Burgess Shale. **a–d**, NMNH 83935 (holotype): in contrast to body tissue, decay fluids lack a sharp margin and are non-reflective; **e–f**, ROM 57776, showing full length of appendage one. Acronyms as in Fig. 1. Scale bars = 5 mm.

Extended Data Figure 7: Hallucigenia *sparsa* (ROM 63146), composite image of part and counterpart. Acronyms as in Fig. 1. Scale bar = 5 mm.

Extended Data Figure 8: *Hallucigenia sparsa* from the Burgess Shale. **a–d**, NMNH 193996: b–c, enlargements of area boxed in a; c, secondary electron micrograph; d, backscatter electron micrograph of region marked in c; **e–g**, ROM 63141, showing position of mouth; **h–j**, ROM 63144; i, secondary electron image of region marked in h; j, backscatter electron image of region marked in i, showing eyes and mouthparts, with interpretative diagram; **k–m**, ROM 63140; l, backscatter SEM of head, showing right eye and mouthparts (enlarged in m, with interpretative diagram). Acronyms as in Fig. 1. Scale bars = 10 mm (k), 5 mm (a, e, h), 1 mm (b-c, l), 0.5 mm (i), 0.1 mm (d, j, m).

Extended Data Figure 9: *Hallucigenia sparsa* from the Burgess Shale. **a**, ROM 43045, cluster of dissociated specimens; **b**, ROM 63145, dissociated specimen showing spines in close anatomical position. Acronyms as in Fig. 1. Scale bars = 10 mm.